



Migration of Excitation Energy in Furocoumarins

O.N. Tchaikovskaya^{1,2*}, N.G. Dmitrieva^{1,3}, E.N. Bocharnikova¹, V.S. Chaidonova^{1,4} and P.V. Avramov^{5*}

¹Laboratory Photophysics and Photochemistry of Molecules, Department of Physics, Tomsk State University, Tomsk, Russia, ²Laboratory of Quantum Electronics, The Institute of Electrophysics of the Ural Division of the Russian Academy of Sciences, Ekaterinburg, Russia, ³Department of Medical Biology, Siberian State Medical University, Tomsk, Russia, ⁴Laboratory of Physical and Chemical Methods, Hygienic and Epidemiological Center in Republic of Khakassia, Abakan, Russia, ⁵Department of Chemistry, Kyungpook National University, Daegu, South Korea

The migration of excitation energy of a number of psoralen compounds has been studied. For this, the methods of induced absorption spectroscopy, stationary electron spectroscopy, fluorescence and phosphorescence, as well as quantum chemistry were used. A comparative photostability of psoralen was achieved by exposure to a XeCl excilamp irradiation (emission wavelength $\lambda_{em} = 308$ nm) with parameters $\Delta\lambda = 5\text{--}10$ nm, $W_{peak} = 18$ mW/cm², $p = 8.1$ J/cm³, $f = 200$ kHz, pulse duration 1 μ s. It was found that the singlet-triplet transition played a major role in the migration of excitation energy into triplet states. Among all tested compounds, substances with an OCH₃-group in the structure have the strongest effect on the spectral-luminescent characteristics.

Keywords: furocoumarin, luminescence, singlet-singlet transition, triplet-triplet transition, photodynamic activity

INTRODUCTION

Due to its sensitivity, fluorescence spectroscopy (Weber et al., 2020; Keuler et al., 2021) has become one of the most commonly used methods in biomedical research. Coumarin-based sensors hold great promise in detecting residual amounts of heavy metals in the body (Wei et al., 2018). Currently, there is an active search for anticancer drugs (Shen et al., 2019; Spreckelmeyer et al., 2018). Due to the unfavorable activity and selectivity of tumor cells, the number of inhibitors is very limited and their effect remains unknown. The authors of the work present studies of an anticancer inhibitor (Bai et al., 2021) based on a coumarin scaffold and low molecular weight phenolic compounds and show its therapeutic effect in the treatment of cancer by disrupting tubulin polymerization. More and more attention is paid to chemotherapy of cancer cells that respond to the redox potential. The chemotherapeutic molecule attaches to the fluorophore through a self-disrupting linker (Odyniec et al., 2019). There is an active search for a “fluorescent linker” that can be both a diagnosis and a therapeutic agent. Such a theranostic prodrug becomes possible to create on the basis of a self-destructive coumarin linker. The wide possibilities for the synthesis of various coumarin derivatives using virtual combinatorial chemistry and spectrophotometry allowed the authors (Rauhamäki et al., 2018) to create a powerful low molecular weight cancer inhibitor based on 3-phenylcoumarin. The new compounds were found to cause >70% inhibition at a concentration of 100 nM to 1 μ M, and 6-methoxy-3-(4-(trifluoromethyl) phenyl)-2H-chromen-2-one at a concentration of approximately 56 nM. At the same time, without any substituents, 3-phenylcoumarin has no biological effect. In (Ibrar et al., 2018), it was shown that in the treatment of Alzheimer’s disease, the effective role of coumarinylthiazoles and oxadiazoles is to inhibit the hydrolysis of acetylcholine in cholinergic

OPEN ACCESS

Edited by:

Rene A. Nome,
State University of Campinas, Brazil

Reviewed by:

Fabio Da Silva Miranda,
Fluminense Federal University, Brazil

Natalya Sultimova,
Emanuel Institute of Biochemical
Physics (RAS), Russia

*Correspondence:

O.N. Tchaikovskaya
tchon@phys.tsu.ru
P.V. Avramov
paul.avramov@gmail.com

Specialty section:

This article was submitted to
Physical Chemistry and Chemical
Physics,
a section of the journal
Frontiers in Chemistry

Received: 09 August 2021

Accepted: 15 October 2021

Published: 04 November 2021

Citation:

Tchaikovskaya ON, Dmitrieva NG,
Bocharnikova EN, Chaidonova VS and
Avramov PV (2021) Migration of
Excitation Energy in Furocoumarins.
Front. Chem. 9:754950.
doi: 10.3389/fchem.2021.754950

synapses, blocking its metabolic activity. Scientists in developed countries are trying to find a solution as soon as possible, working on the creation of vaccines and antiviral drugs. The authors (Yañez et al., 2021) evaluated compounds of coumarin and quinoline derivatives as promising SARS-CoV-2 Mpro inhibitors.

Furocoumarins are heterocyclic aromatic compounds resulting from the condensation of a furan ring with a coumarin ring (Gasparro, 1996), as well as classic chemical compounds with phototoxic properties that naturally occur in many plants (Dolan et al., 2010; Wagstaff, 1991). Furocoumarins have attracted close attention of researchers in recent decades due to their photoactivity. Contact with exposure to ultraviolet radiation can lead to skin burns, a reaction known as phytophotodermatitis (Lagey et al., 1995). The emergence of phytophotodermatitis among therapeutic agents to increase melanin production and improve resistance to sunlight (Scott et al., 1976). Furocoumarins have also been used to treat vitiligo, psoriasis, and other skin conditions with psoralen and ultraviolet (or PUVA) therapy (Parrish et al., 1974; Stern, 2012). Furocoumarin therapy involves topical or oral administration of a furocoumarin derivative, usually 8-methoxypsoralen, followed by irradiation for 1–2 h with near-UV light (about 320–400 nm). These compounds are of particular interest because they have good spectral characteristics capable of accumulating in tissues in high qualities, as well as, in most cases, high photodynamic activity, which allows them to be used as promising photosensitizers for biology and medicine. Using these opportunities for use. Interestingly, due to the ability of furocoumarins to interact and disrupt DNA replication, there is great interest in the development of anti-cancer therapies. Early *in vitro* studies have already shown that furocoumarins can inhibit the growth of various cell types, including cancer and non-small cell lung cancer (Mi et al., 2017; Panno and Giordano, 2014; Wrześniok et al., 2017). These results suggest that if they can target cancer cells *in vivo*, furocoumarins could be a potential therapeutic agent for some cancers.

Complex photophysical, photochemical and biological mechanisms are based on photodynamic action through compounds, but it is obvious that the first stage is determined by the photophysical processes occurring in molecules and leading to the effective population of triplets. In practice, it is necessary to select the more suitable optimal compounds for a particular medical treatment, and to minimize their effects on the body. The effects of furocoumarin on human health remain complex, and there are still many questions regarding the safety of their medicinal use and their consumption with food.

OBJECTS AND METHODS OF RESEARCH

Objects

In the work, as objects of research, we used substances with chemical purity (99.8%) from Aldrich, Code: 56448: 8-methoxypsoralen (8-MOP); and also considered a number of objects for research with a chemical purity of 99.7% (Garazd et al., 2002; Garazd et al., 2006): 3,4-phenyl-4', 5'-cyclohexylpsoralen

(KC3), 4'-methyl, 3,4-cycloheptylpsoralen (KC4), 4', 5'-dimethyl-3,4 -cyclohexylpsoralen (KC5). The structural formulas of all studied compounds are shown in **Figure 1**. We have given simple usual structures of the objects under study in the **Supplementary Material**.

Aldrich ethanol C₂H₅OH with chemical grade (99.9%) was used as a solvent. The experiments on absorption from the ground state, fluorescence, and induced absorption were carried out at room temperature 20°C and a pressure of 760 mm Hg. The phosphorescence experiment was carried out at a temperature of 77 K.

Equipment

The obtained characteristics of 8-MOP were interpreted in comparison with the data for KC3, KC4, and KC5 molecules. The compounds under study are readily soluble in organic solvents and poorly soluble in water. The spectral-luminescent characteristics of the solutions were recorded on a CM2203 spectrofluorimeter (SOLAR, Belarus), an Evolution-600 spectrophotometer (Thermo Scientific), and a Cary Eclipse spectrofluorimeter (Varian) with an Optistat DN cryostat. To measure the spectra of induced absorption, we used a setup based on the pump-probe method.

Research Methods

The study of the spectral-luminescent properties of substituted coumarins was carried out using an integrated approach combining experimental and theoretical consideration of the spectral-luminescent properties. The phosphorescence quantum yields were determined using the method of comparison with the standard. 8-MOP was chosen as a standard, emitting in a close spectral region; its phosphorescence quantum yield at 77 K in ethanol is 0.17 (Mantulin and Song, 1973). The concentration of the substances under study in solutions was selected such that the optical density at the excitation wavelength (330 nm) was 0.1.

To study the spectra of induced absorption, we used an experimental setup designed to record the spectra of nonstationary differential absorption by the pump-probe method with a fluorescent probe. The setup provided nanosecond time resolution. Its optical design, principle of operation and signal processing are given in (Svetlichnyi, 2010). The setup makes it possible to separate the absorption spectra of short-lived states and products, for example, singlet-singlet ($S_1 \rightarrow S_n$) absorption and long-lived (longer than the pump pulse duration), for example, triplet-triplet ($T_1 \rightarrow T_m$) absorption of molecules. Pumping was performed by the third (355 nm) harmonic of a pulsed Nd: YAG laser with Q-switching, $\tau_{1/2} = 7$ ns, $E_{\text{imp}} = 20 \div 40$ mJ. The fluorescence of a mixture of dye solutions (range 350–750 nm, luminescence duration 9 ns), excited by the same pump laser, was used as the probe radiation. The delay line was 10 m, which corresponds to a delay time of about 30 ns. The concentration of the investigated solutions for the experiment with a pumping probe was chosen to be 0.01 mM, while the optical density (OD) at the pump wavelength is in the range of 0.07–0.18 relative units.

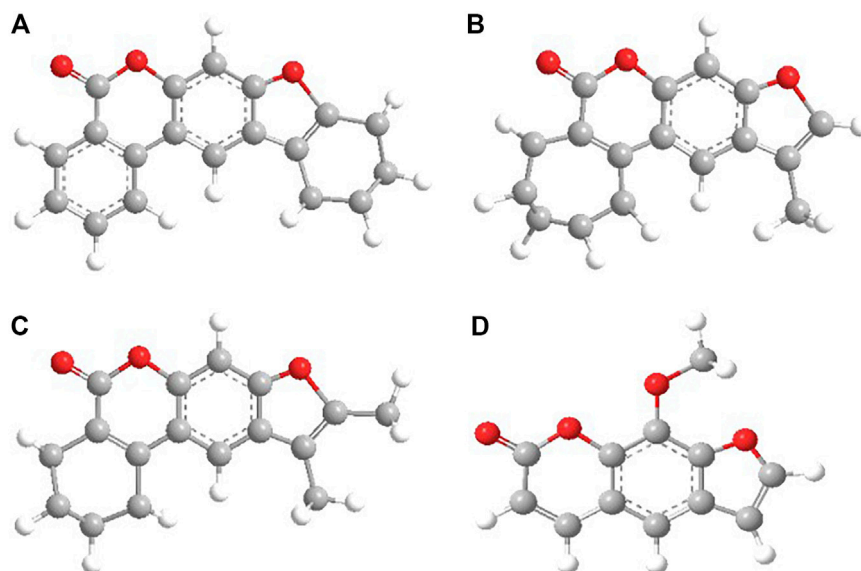


FIGURE 1 | Chemical structures of the studied molecules: **(A)** KC3; **(B)** KC4; **(C)** KC5; **(D)** 8-MOP.

The Photostability of the Compounds

To study of compounds photostability could provide information about their preservation. The solutions of substituted coumarins were irradiated in quartz cells with an optical layer thickness of 1 cm. As a source of UV radiation for photochemical studies, we used a U-type exciplex barrier discharge exciplex lamp based on working Xe and Cl* molecules ($\lambda_{em} = 308$ nm) with parameters $\Delta\lambda = 5\text{--}10$ nm, illumination power density 18 mW/cm², volumetric energy dose 8.1 J/cm³, pulse repetition rate 200 kHz, pulse duration 1 μ s. The intensity of the light source $I = 4 \times 10^{15}$ photons/s was determined by the method (Calvert and Pitts, 1966; Becker, 1976). The irradiation time varied from 2 to 32 min. Changes in the characteristics of substituted coumarins were monitored simultaneously by spectrophotometric and fluorescence methods on a CM2203 spectrofluorimeter (the device allows recording both fluorescence and absorption spectra). For experimental studies, ethanol solutions of the studied compounds with a concentration of 0.1 mM were prepared.

Calculations

In the 60–70 s of the 20th century, a large number of semiempirical methods were created based on the zero differential overlap approximation. In semiempirical methods, the main part of the molecular integrals of the Coulomb repulsion is neglected. In addition, the core integrals are usually not calculated exactly, but are replaced by parameters that are calibrated so as to either obtain the best agreement between the calculated and experimental characteristics, or to achieve agreement with ab initio calculations, when the values of the group of physical properties and quantities calculated by this method are good enough. Most often, semiempirical methods use the valence approximation, according to which only electrons and the corresponding valence shell orbitals are taken into account in

the LCAO MO expansion; internal electrons, for example, $1s$ carbon and other elements of the second and higher periods, are considered to be localized in the corresponding atomic orbitals and form an unpolarized core. Semiempirical methods are quite simple and are applied to the calculation of large molecules on modern computers.

In this work, a set of quantum-chemical programs is used, which makes it possible to correctly and reliably solve the assigned tasks and obtain a fairly good agreement ($\sim 5\text{--}10\%$) with the available experimental spectral data. And, most importantly, the software package that we have chosen made it possible to interpret the available experimental data and opened up the possibility of predicting the behavior of molecular structures in advance. Since theoretical studies of the molecular photonics of furocoumarins showed the low efficiency of the “standard” calculation methods, therefore, a set of quantum-chemical programs was used to study them, the basis of which is the semiempirical method of intermediate neglect of differential overlap (INDO) with original spectroscopic parametrization (Alfimov and Galeeva, 1986). The method has been successfully developed for a long time for the correct calculation of the spectral and luminescent properties of polyatomic organic molecules. Over the past 30 years, this package has been intensively used to study the photonics of polyatomic organic molecules. Using the software package, you can determine the important characteristics of the electronic states of polyatomic molecules: the energies and nature of molecular orbitals, the energies and wave functions of singlet and triplet electronically excited states, the oscillator strength and polarization of electronic transitions, the distribution of the electron density on the atoms and bonds of the molecule, the dipole moments in ground and excited states, rate constants of radiative and nonradiative processes involving electronically excited states of molecules, as well as absorption spectra from

excited singlet and triplet states (Artyukhov et al., 2008; Alfimov et al., 2014; Artyukhov et al., 1997; Plotnikov, 1979; Pomogaev and Artyukhov, 2001). Moreover, this software set has achieved success in solving the problems of large molecules photonics (Plotnikov, 1979; Artyukhov and Pomogaev, 2000; Bocharnikova et al., 2019; Liano et al., 2003; Reveguk et al., 2020; Tchaikovskaya et al., 2020). The methodology for studying the spectral-luminescent properties of complex molecules was described in (Alfimov and Plotnikov, 2014; Bocharnikova et al., 2020). In order to construct a diagram of electronically excited states of furocoumarins, the geometry was optimized by the quantum-chemical method AustinModel 1 (Austin model 1 or AM1) (Dewar Michael, 2012; Quirante, 1995). The exact structural parameters of the studied molecules (bond lengths, bond and torsion angles) are unknown; therefore, the geometry of the ground state was carefully optimized by the method of molecular mechanics (MM2) from the popular Chem Office software program (Blatov et al., 2005). The ChemDraw Ultra was used to create a spatial model of the molecular structure. The geometry optimization method AM1 was determined using the Chem3D Ultra and HyperChem programs (ChemOffice, 2000; HyperChem 7.0, 2021).

The calculation of the Cartesian coordinates of atoms in furocoumarin molecules was performed using the moco02.exe program. As the initial data, quantitatively determining the spatial structure of the molecule, we used the values of the lengths of chemical bonds, bond and torsion angles (angles of rotation) (Artyukhov and Pomogaev, 2000). The indo02.exe program was used to calculate the electronic structure and spectra of polyatomic molecules by the INDO method. This made it possible to take into account only the valence electrons of the atoms that make up the molecule. The revue02.exe program was used to calculate the rate constants of intramolecular radiative and nonradiative processes and the quantum yield of fluorescence (Artyukhov and Pomogaev, 2000). The K_{ST} .exe program was used to calculate the rate constants of the intercrossing conversion (Artyukhov and Pomogaev, 2000). Absorption spectra from excited states provide information on high-lying energy levels and photoprocesses involving such states (Artyukhov and Mayer, 2012; Artyukhov and Maier, 2001; Artyukhov and Galeeva, 1986).

RESULTS

Spectral-Luminescent Characteristics

For the investigated series of molecules: KC3, KC4, KC5, 8-MOS (see **Figure 1**) spectral-luminescent characteristics were obtained. **Figure 1** shows that 8-MOP has been a high electron localized in the S_0 state than KC3 and KC5. In the **Supplementary Material**, changes in electron density redistribution for furocoumarins have been reported. The oxygen atom of the carbonyl group of 8-MOP, KC3, and KC4 plays an important role in charge transfer during the transition from the S_0 to the S_3 state upon excitation. The carbonyl group of furocoumarins participate in intermolecular interactions. Quantum-chemical calculations have shown that the oxygen atom of KC5 carbonyl group is less involved in the

redistribution of the effective charge than 8-MOP. **Figure 2** shows the fundamental laws, namely the normalized spectra: absorption, fluorescence, phosphorescence, induced absorption of the compounds under study.

Figure 2 shows that the maximum of the long-wavelength absorption band for compounds KC3 and KC5 is located at 332–334 nm (see **Figures 2A,C**), the maximum of the short-wavelength band for the entire group of compounds lies in the region of 245–250 nm, for 8-MOP the maximum of the long-wavelength band is at 302 nm (see **Figure 2D**). The maximum of the fluorescence spectra for the whole series of studied compounds falls on the 420–488 nm region: for compounds KC3 and KC5 is located at 488 and 438 nm (see **Figures 2A,C**); for KC4 and 8-MOP—at 422 and 468 nm (see **Figure 2**), respectively. The experimental maximum of phosphorescence for a substituted coumarins falls on the long-wavelength range of 455–513 nm. The maximum of the phosphorescence spectra for KC3 falls on 452 nm, for KC4—513 nm, for KC5—496 nm and for 8-MOP—495 nm, respectively (see **Figure 2**). The maximum of the spectra of induced absorption lies in the region of 370–435 nm. The maximum of the spectra of induced absorption lies for KC3 falls on 377 nm, for KC4—425 nm, for KC5—430 nm and for 8-MOP—360 nm, respectively (see **Figure 2**). The experimental data are consistent with the data obtained using quantum-chemical calculations (see **Table 3**). According to the data of quantum-chemical calculations, the appearance of these bands in the spectra is due to triplet-triplet transitions. However, in the spectra of induced absorption there are bands in the region of 650 nm. This band is very well registered for 8-MOS (see **Figure 2D**) and not explicitly for other molecules. It can be assumed that this streak is associated with the appearance of the spice.

Diagrams of Electronically Excited States

Figure 3 demonstrates the distribution of the effective charge in molecules over fragments using quantum calculations. Delocalization of the effective charge was observed for the 8-MOS molecule. It is shown (see **Table 1**) that all the compounds studied absorb in one spectral region: the experimental long-wavelength band is located in the region of 332–334 nm. The nature of the first excited singlet state is of the $\pi\pi^*$ -type for all compounds, and the second excited singlet is predominantly of the $n\pi^*$ -type, or of a mixed type. There is some change in the dipole moment of the systems under study, depending on the structure of the studied substituted coumarin. The $S_0 \rightarrow S_1$ transition occurs to states of the $\pi\pi^*$ type, for which we observe the largest values of the dipole moments. The dipole moment of the singlet S_2 states of the $n\pi^*$ -type nature is less in comparison with the states of the $\pi\pi^*$ -type nature. Comparing the experimental and theoretical values of the wavelengths for a number of studied compounds, we note good agreement between the data.

Table 2 shows the data on luminescence and the values of Stokes shifts for all objects of this study.

Stokes Shift

It can be seen from **Table 2** that the values of fluorescence quantum yields obtained experimentally for a number of

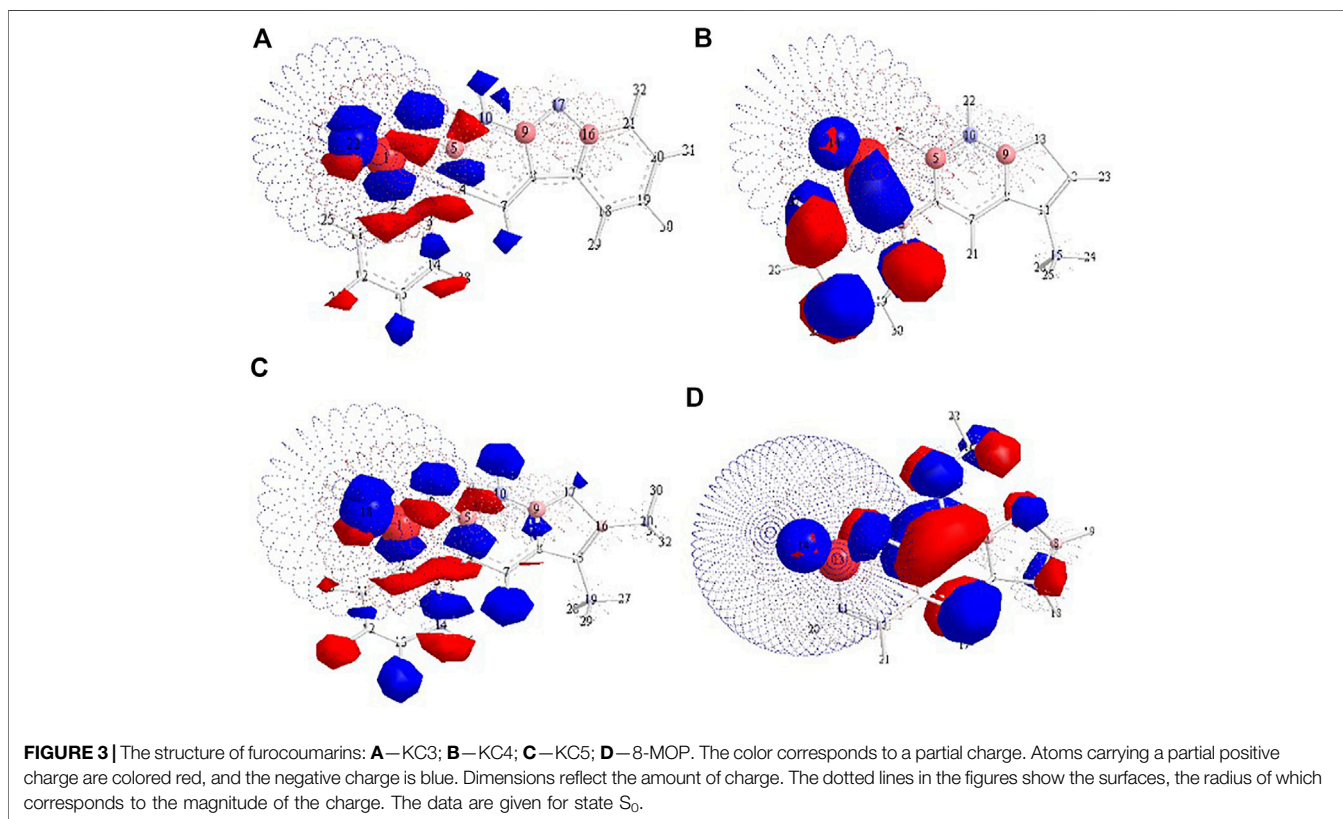
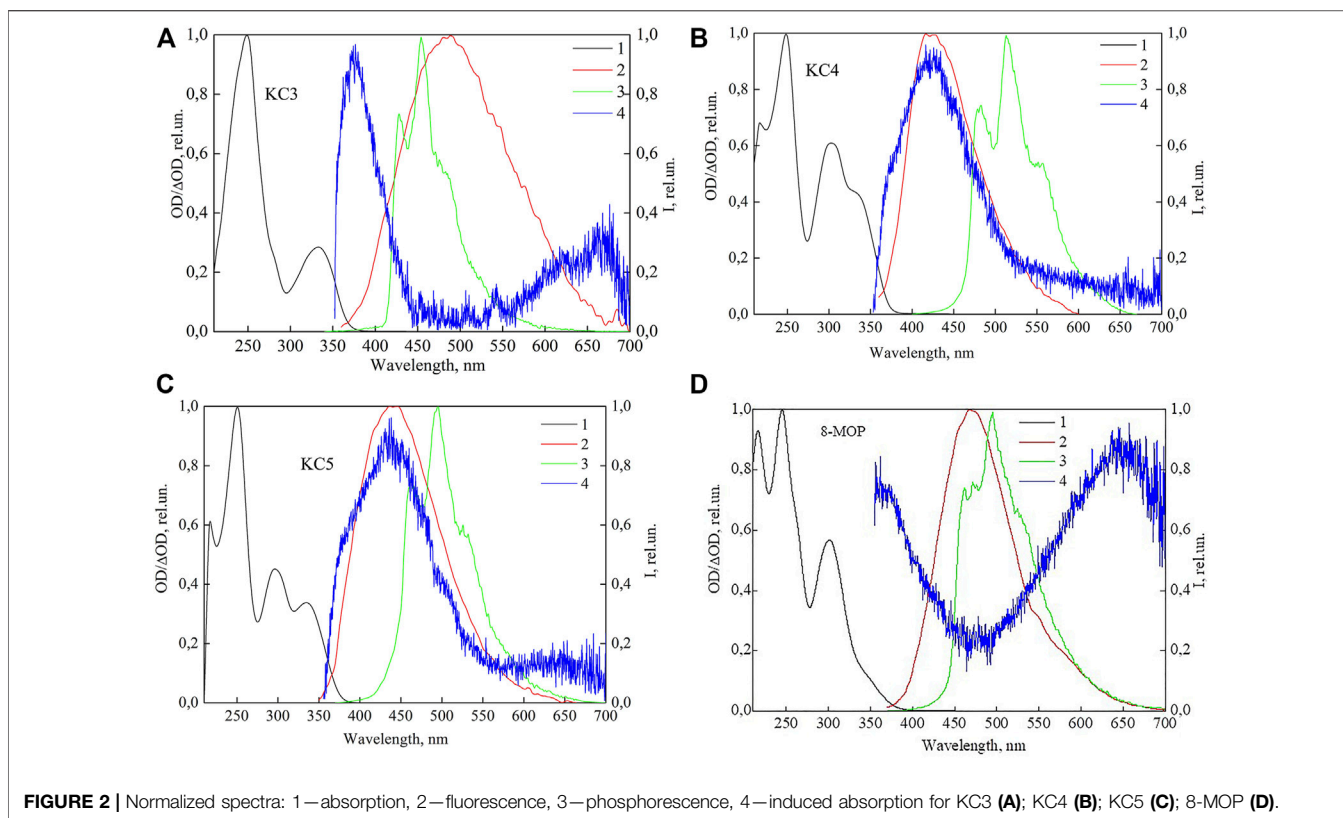


TABLE 1 | Singlet-Singlet absorption spectra of several compounds.

Object	Quantum chemical calculations data					Experimental
	Transition	Energy, E_f , cm^{-1} (nm)	Oscillator strength, f	Dipole moment, d	Orbital type of the transition	λ , nm
KC3	$S_0 \rightarrow S_1$	30700 (326)	0.46	8.29	$\pi\pi^*$	332
	$S_0 \rightarrow S_2$	33000 (303)	0.00	3.39	$n\pi^*$	-
	$S_0 \rightarrow S_5$	35100 (285)	0.13	8.47	$\pi\pi^*$	282
	$S_0 \rightarrow S_8$	39700 (252)	0.25	8.87	$\pi\pi^*$	246
KC4	$S_0 \rightarrow S_1$	30200 (331)	0.51	7.89	$\pi\pi^*$	332
	$S_0 \rightarrow S_2$	33300 (300)	0.12	7.45	$n\pi^* + \pi\pi^*$	301
	$S_0 \rightarrow S_7$	40300 (248)	0.47	8.62	$\pi\pi^*$	252
KC5	$S_0 \rightarrow S_1$	30200 (331)	0.39	9.54	$\pi\pi^*$	334
	$S_0 \rightarrow S_2$	33100 (302)	0.00	3.29	$n\pi^*$	-
	$S_0 \rightarrow S_3$	34100 (293)	0.09	8.53	$\pi\pi^* + \sigma\pi^*$	296
	$S_0 \rightarrow S_7$	39100 (256)	0.33	9.04	$\pi\sigma^*$	252
8-MOP	$S_0 \rightarrow S_1$	31700 (316)	0.08	8.92	$\pi\pi^*$	332
	$S_0 \rightarrow S_2$	33600 (297)	0.00	3.36	$n\pi^*$	301
	$S_0 \rightarrow S_3$	34100 (294)	0.19	6.56	$\pi\pi^*$	-
	$S_0 \rightarrow S_7$	40500 (245)	1.13	10.39	$\pi\sigma^*$	245

TABLE 2 | Luminescence quantum yields of the compounds.

Object	Fluorescence quantum yield of, φ_f		Experimental data			
	Theoretical	Experimental	Fluorescence wavelength, λ_{fl} , nm	Stokes shift, cm^{-1}	Phosphorescence	
					λ_{ph} , nm	Quantum yield, φ_{ph}
KC3	0,009	0,036	488	8900	452	0,71
KC4	0,031	0,029	422	6500	513	0,26
KC5	0,003	0,059	438	7600	496	0,45
8-MOP	0.001	0,0013	468, 470 Lai et al. (1982)	12200	495	0,19

studied systems are in good agreement with the data of quantum-chemical calculations by the AM1 method. For all investigated substituted coumarins: KC3, KC4, KC5, 8-MOP, a significant Stokes shift of $6,500 \div 12,200 \text{ cm}^{-1}$ is observed. The largest value of the Stokes shift corresponds to the substance 8-MOP. This value can be associated with changes in the geometry of molecules in excited singlet states. From the experimental and theoretical data, it can be seen that all the investigated substituted coumarins are weakly fluorescent. It can be seen from the literature that for the known furocoumarins, the experimental values of the fluorescence quantum yields are in good agreement with the data for compounds with a related structure (for psoralen- $\varphi_{fl} = 0.01 \div 0.023$, for 8-MOP- $\varphi_{fl} = 0.0013$ (Mantulin and Song, 1973)). Compound KC3 has the highest phosphorescence quantum yield - 0.71. The information on the position of the bands and the quantum yields of fluorescence and phosphorescence of 8-MOP that we obtained is consistent with the literature data ($\lambda_{fl} = 470 \text{ nm}$, $\lambda_{ph} = 457 \text{ nm}$, $\varphi_{ph} = 0.17$) (Mantulin and Song, 1973; Lai et al., 1982).

Next, we studied the absorption spectra from excited states, due to the fact that they are informative from the point of view of

obtaining data on the structure of energy levels and photoprocesses involving such states.

Induced Absorption Spectra

Experimental induced absorption was found for a group of investigated compounds: KC3, KC4, KC5, 8-MOP, and theoretical T_1-T_i absorption spectra were calculated by the quantum-chemical method (see Table 3). Analysis of the data shows that for all substituted furocoumarin molecules containing phenyl and cyclohexyl substituents (KC3), cycloheptyl and methyl radical (KC4), cyclohexyl and two methyl radicals (KC5), or methoxy group (8-MOP), T-T absorption spectra have some differences.

It can be seen from the table that the T_1-T_{13} , T_1-T_{15} , T_1-T_{12} transitions for the KC4, KC5 and 8-MOP molecules, respectively, are recorded in a longer wavelength region of the spectrum compared to the T_1-T_{24} KC₃ transition.

It is known from the literature that for an unsubstituted furocoumarin molecule the absorption maximum in benzene coincides with the absorption maximum in water. According to the data of (Parrish et al., 1974; Bethea et al., 1999), when

TABLE 3 | Triplet-Triplet absorption spectra of several compounds.

Method	Compound							
	KC3		KC4		KC5		8-MOP	
	λ , nm (T ₁ -T ₁)	Oscillator strength, <i>f</i>	λ , nm (T ₁ -T ₁)	Oscillator strength, <i>f</i>	λ , nm (T ₁ -T ₁)	Oscillator strength, <i>f</i>	λ , nm (T ₁ -T ₁)	Oscillator strength, <i>f</i>
Calculation	377 (T ₁ -T ₂₄)	0,08	425 (T ₁ -T ₁₃)	0,014	430 (T ₁ -T ₁₅)	0,01	471 (T ₁ -T ₁₂)	0,01
	330 (T ₁ -T ₃₀)	0,08	384 (T ₁ -T ₁₄)	0,032	386 (T ₁ -T ₁₈)	0,01	327 (T ₁ -T ₂₀)	0,02
	317 (T ₁ -T ₃₂)	0,21	321 (T ₁ -T ₂₀)	0,225	331 (T ₁ -T ₂₃)	0,19	300 (T ₁ -T ₂₄)	0,26
Experiment	377	-	425	-	430	-	360	-

TABLE 4 | Rate constants of photophysical processes^a of lower singlet excited states. The geometry of the molecular structure was optimized by the AM1.

Compound	k_r , s ⁻¹	k_{IC} , s ⁻¹	k_{ST} , s ⁻¹
8-MOP	5.7×10^7	5.8×10^3	3.4×10^{10}
KC3	1.4×10^8	1.4×10^3	1×10^{10}
KC4	1.4×10^8	2.7×10^3	1×10^9
KC5	1.0×10^8	3.4×10^3	1×10^9

^aWhere k_r , is the rate constant of radiation; k_{IC} , is the rate constant of internal conversion; k_{ST} , is the rate constant of the intersystem crossing process.

passing from methanol to benzene, the T-T absorption spectrum of furocoumarin shifts by 10 nm to the red region.

Experimentally, the spectra of induced absorption were obtained for all studied compounds, the maxima of which are at 374, 425, 438, and 456 nm for KC3, KC4, KC5, 8-MOS, respectively. Due to the fact that the probe radiation lies in the long-wavelength region of the spectrum (350–700 nm), the transitions T₁-T₃₂ for KC3, T₁-T₂₀ for KC4, T₁-T₂₃ for KC5 and T₁-T₂₄ for 8-MOP were not recorded with using an experimental setup.

Transitions T₁-T₂₄ and T₁-T₃₀ for connecting KC3, T₁-T₁₃ and T₁-T₁₄ for connecting KC4, T₁-T₁₅ and T₁-T₁₈ for connecting KC5, T₁-T₁₂ and T₁-T₂₀ for an 8-MOP connection are carried out between the states of one nature ($\pi\pi^*$ - $\pi\pi^*$), and the transitions T₁-T₃₂, T₁-T₂₀, T₁-T₂₃, T₁-T₂₄ for compounds KC3, KC4, KC5, 8-MOP, respectively, between states of different orbital nature ($\pi\pi^*$ - $\pi\sigma^*$). This explains the reason for the more intense triplet-triplet absorption in the region of 317–331 nm. Comparing the results of experimental and quantum-chemical studies, we note good agreement for the long-wavelength T₁-T₂₄, T₁-T₁₃, T₁-T₁₅, and T₁-T₁₂ transitions of substituted coumarins KC3, KC4, KC5, and 8-MOP, respectively.

The Channels of Degradation of the Excitation Energy

Due to the fact that compounds fluoresce weakly, it is considered what happens with the energy further, for this, the rate constants of radiation, internal and intersystem conversions were calculated using the quantum-chemical method. The values of the rate constants for the photophysical processes occurring in the compounds under study are shown in **Table 4**.

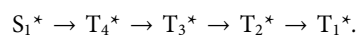
It was found that, for the entire series of substituted coumarin studied, there is an effective intercombination conversion with

large rate constants $\sim 10^{10} \div 10^{11} \text{ s}^{-1}$ due to the close arrangement of levels having different orbital nature of the $\pi\pi^*$ and $\pi\sigma^*$ types, which led to small values of quantum yields fluorescence and, consequently, to a significant population of the triplet state.

After optimization of the geometry by the AM1 method (see **Figure 4**) and quantum-chemical calculation, schemes of electronically excited states were constructed and the rate constants of photophysical processes were estimated. From the results obtained, we can say that there is good agreement between the calculated and experimental data. Let's consider the ways of deactivation of energy in more detail.

Energy level diagrams represent the main processes that occur in molecules after absorption of radiation. The figure shows the most effective rate constants of internal and intercombination conversions, as well as the radiation constants. An analysis of the electronically excited state diagrams showed that, for the compounds studied, the lower singlet electronically excited state S₁ has the orbital nature of the $\pi\pi^*$ -type and the S₂ state, predominantly of the $\pi\pi^*$ -type. For the group of compounds under study, the singlet S1 is located in the region of 316–331 nm, which is in good agreement with the experimental data (they are shown by dashed lines): 331–334 nm (see **Table 1**) Electronic singlet-singlet transitions of the $\pi\pi^*$ -type in the lower singlet excited state S₁ and in the S₃ state are formed mainly by carbon atoms, and the $\pi\pi^*$ -type transitions are formed by carbonyl oxygen atoms for the entire group of the studied substituted coumarins. The low value of the quantum yield of fluorescence is determined by the high values of the rate constants of nonradiative processes in comparison with radiative decay. This explains the high values of phosphorescence quantum yields (0.19–0.71), which were obtained as a result of experimental studies at the facility.

The intersystem conversion process is the main channel for degradation of the excitation energy ($k_{ST} \sim 10^{10} \text{ s}^{-1}$) for the entire group of substituted coumarins. The high value of the intersystem conversion constant is due to the close location of the $\pi\pi^*$ -type singlet state and the $\pi\sigma^*$ -type triplet state. **Figure 3** shows that the channels of degradation of the excitation energy in the 8-MOP complex have one main channel through the system of triplet states, following one after the other:



KC3 has the following main channel for degradation of the excitation energy:

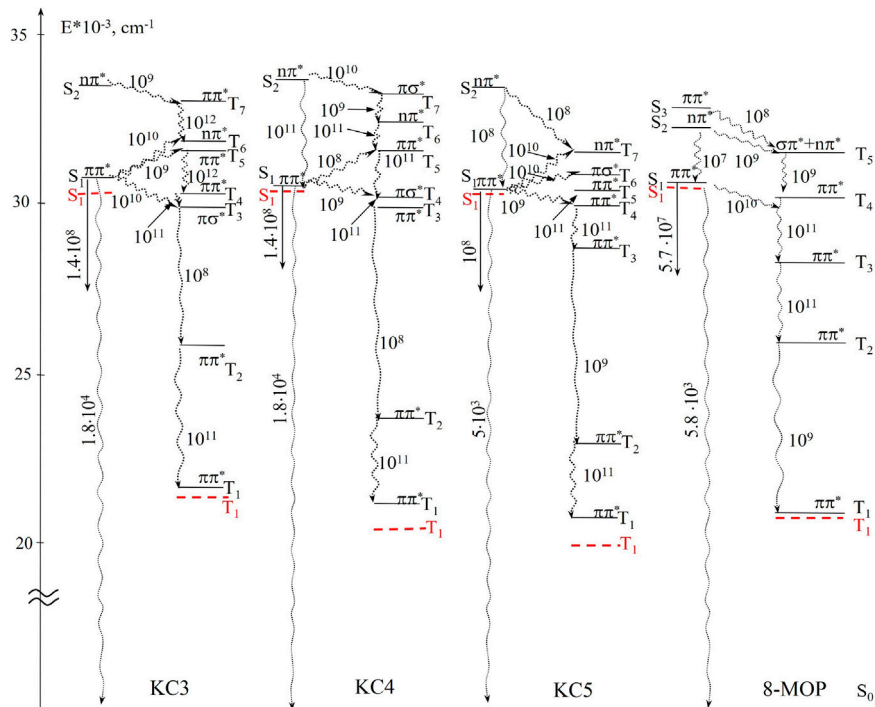
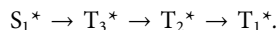
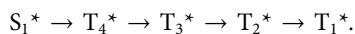


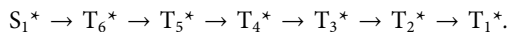
FIGURE 4 | Diagrams of electronically excited states of the compounds (dashed lines indicate experimental values). Arrows show the ways of energy relaxation, the numbers near them are the rate constants of these processes, s^{-1} .



KC4 has one main channel for degradation of the excitation energy:



KC5 has the following main channel for degradation of the excitation energy:



It can be seen from the diagram that for the investigated series of substituted coumarins, the nature of the T_1 state is of the $\pi\pi^*$ -type. Taking into account the data (nature and rate of intersystem crossing conversion), it can be concluded that the studied compounds are effective $\pi\pi^*$ -sensitizers. For the studied compounds, good agreement was obtained between the calculated and experimental data for all interpreted bands, which confirms the possibility of using the calculation scheme for interpreting the spectra.

Photostability

Quantum yields of photodegradation calculated by the formula (Becker, 1976):

$$\gamma = \frac{D_u - D_t}{D_u} \cdot C \cdot 10^{-3} N_A$$

$$I \cdot t$$

TABLE 5 | Absorbance intensity and photodecay quantum yield of compounds under the irradiation of XeCl* excilamp.

Irradiation time, min	Compounds			
	KC3	KC4	KC5	8-MOP
	Absorbance intensity, relative units			
0	0.750	0.713	0.738	0.733
2	0.697	0.688	0.678	0.704
4	0.653	0.668	0.625	0.688
8	0.591	0.603	0.550	0.646
16	0.485	0.523	0.467	0.568
32	0.343	0.438	0.385	0.472
Photodecay quantum yield	0.004	0.007	0.006	0.004

where D_u and D_t —optical density of unirradiated and irradiated solutions, rel. un.; C —concentration of solution, M; N_A —Avogadro's number, $6,022 \cdot 10^{23} \text{ mole}^{-1}$; I —irradiation intensity, photon/s; t —exposure time, s.

Due to the fact that photostability is an important property for a wide variety of applications, we studied the effect of radiation from a lamp source on the spectral-luminescent properties of a number of substituted coumarins (see **Table 5**). The dependence of the optical density on the irradiation time is obtained. Analysis of the data in **Table 5** showed that, after 30 min of excilamp irradiation, the highest phototransformation efficiency was recorded for KC3.

The optical absorption density for KC3 dropped from 0.750 to 0.343. This indicates that more than 50 percent of the KC3 molecules are photodegraded. However, it should be noted that the values of the quantum yield of photodecay turned out to be low—less than 0.01 and did not give correct agreement with the number of decayed molecules.

The effect of XeCl* excilamp irradiation on the photostability of the investigated series of substituted furocoumarins was evaluated. Note that the change in optical density was recorded at the wavelength of the absorption maximum of the unirradiated solution, namely: the wavelength of the absorption maximum for KC3 and KC4 is 332 nm, for KC5 – 334 nm, and for 8-MOP – 302 nm. Radiation of 308 nm falls into the region of long-wave absorption of the entire group of compounds studied, more precisely, into the S₂-state. Therefore, upon irradiation with an excilamp, direct photolysis of the molecule can occur in the system. The calculated quantum yields of photodegradation of a number of substituted furocoumarin show that all compounds are highly photostable. The mechanism of photosolvolysis is known from the literature, according to which the primary stage is a nucleophilic attack of a solvent molecule on 4' or 5' carbon atoms of furocoumarin in an excited state (Caffieri, 2002). In the case of KC3, KC4, and 8-MOP, the methyl and methoxy groups sterically hinder the addition of the solvent and reduce the reactivity of the substrate due to an increase in the electron density at the reaction center. As for the KC3 compound, it is also possible for it to break the 4'-5' bond.

CONCLUSION

Based on the data obtained as a result of optimization of the geometry of molecules by the AM1 method and quantum-chemical calculation by the NPDP/s method, a diagram of the electronically excited states of the compounds under study is constructed. Thanks to this scheme, it was found that a number of substituted coumarins are characterized by effective intersystem crossing ($\sim 10^{10} \div 10^{11} \text{ s}^{-1}$). The presence of such constants is explained by the close arrangement of levels with different orbital nature of the $\pi\pi^*$ and $n\pi^*$ -types. The values of the quantum yields of fluorescence (0.0013–0.059) and phosphorescence ($\sim 0.19 \div 0.71$) were determined, which were explained using the scheme of electronically excited states. The triplet-triplet absorption spectra of the studied series of substituted coumarin are calculated. The states involved in the formation of these spectra have been established. The calculated quantum yields of photodegradation of a number of substituted furocoumarin

REFERENCES

- Alfimov, M. V., Plotnikov, V. G., Smirnov, V. A., Artyukhov, V. Y., and Maier, G. V. (2014). Exciplexes in Highly Excited Triplet States. *High Energ. Chem.* 48 (3), 174–179. doi:10.1134/S0018143914030023
- Artyukhov, V. Ya., and Maier, G. V. (2001). Quantum-Chemical Theory of Electronic Excitation Energy Transfer in Molecular Systems. *Russ. J. Phys. Chem. A.* 75 (6), 1034–1040.
- Artyukhov, V. Y., Galeeva, A. I., Maier, G. V., and Ponomarev, V. V. (1997). Processes of Internal Conversion in Polyacenes. *Opt. Spectrosc.* 82 (4), 520–523.
- Artyukhov, V. Y., and Galeeva, A. I. (1986). Spectroscopic Parametrization of the Method of PNDO. *Soviet Phys. J.* 29, 949–952. doi:10.1007/BF00898453
- Artyukhov, V. Y., Kopylova, T. N., Samsonova, L. G., Selivanov, N. I., Plotnikov, V. G., Sazhnikov, V. A., et al. (2008). A Combined Theoretical and Experimental Study on Molecular Photonics. *Russ. Phys. J.* 51 (10), 1097–1111. doi:10.1007/s11182-009-9144-4
- Artyukhov, V. Y., and Mayer, G. V. (2012). Intermolecular Interactions and Photoprocesses in Molecular Systems. *Russ. Phys. J.* 55 (7), 835–842. doi:10.1007/s11182-012-9887-1
- Artyukhov, V. Y., and Pomogaev, V. A. (2000). Three-Center Integrals of One-Electron Operator of a Spin-Orbit Interaction. *Russ. Phys. J.* 43 (7), 590–600. doi:10.1007/BF02508964

show that all compounds have high photostability (0.004÷0.007). It should be noted that the calculated data are in good agreement with the data obtained during the experiments. The main channel for deactivation of the excitation energy in a number of substituted coumarins is singlet-to-triplet state conversion and then a decay through a system of triplet states in 8-MOP: S₁* → T₄* → T₃* → T₂* → T₁*; in KC3: S₁* → T₃* → T₂* → T₁*; in KC4: S₁* → T₄* → T₃* → T₂* → T₁*; in KC5: S₁* → T₆* → T₅* → T₄* → T₃* → T₂* → T₁*.

DATA AVAILABILITY STATEMENT

The original contributions presented in the study are included in the article/**Supplementary Material**, further inquiries can be directed to the corresponding author.

AUTHOR CONTRIBUTIONS

OT and PA conceived the project. ND, EB, VC, and OT designed and performed the experiments. OT, ND, and PA, analyzed the data. EB calculated the data. ND, and EB designed figures. OT, ND, and VC wrote the article.

FUNDING

This study was supported by the collaborative NRF-RFBR grant (Russian project No.19-53-51005 NIF_a RFBR-Korea and Korean ID: NRF-2019K2A9A1A06100125).

ACKNOWLEDGMENTS

OT would like to thank Dr. Valery Svetlichny for providing the setup, which made it possible to obtain the spectra of induced absorption. We also thank Prof. Alexei Kononov for helpful discussions.

SUPPLEMENTARY MATERIAL

The Supplementary Material for this article can be found online at: <https://www.frontiersin.org/articles/10.3389/fchem.2021.754950/full#supplementary-material>.

- Bai, G., Zhao, D., Ran, X., Zhang, L., and Zhao, D. (2021). Novel Hybrids of Podophyllotoxin and Coumarin Inhibit the Growth and Migration of Human Oral Squamous Carcinoma Cells. *Front. Chem.* 8, 626075. doi:10.3389/fchem.2020.626075
- Becker, H. G. O. (1976). *Photochemie*. Berlin: Deutscher Verl. der Wiss, 468.
- Bethea, D., Fullmer, B., Syed, S., Seltzer, G., Tiano, J., Rischko, C., et al. (1999). Psoralen Photobiology and Photochemotherapy: 50 Years of Science and Medicine. *J. Dermatol. Sci.* 19 (2), 78–88. doi:10.1016/S0923-1811(98)00064-4
- Blatov, V. A., Shevchenko, A. P., and Perysheva, E. V. (2005). *Semi-Empirical Calculation Methods of Quantum Chemistry: A Textbook [in Russian]*. Samara: Publishing House "Univer-Grupp, 32.
- Bocharnikova, E. N., Tchaikovskaya, O. N., Artyukhov, V. Y., and Dmitrieva, N. G. (2019). Nature of Electronically Excited States of Furocoumarins. *Russ. Phys. J.* 61 (11), 2033–2041. doi:10.1007/s11182-019-01634-x
- Bocharnikova, E. N., Tchaikovskaya, O. N., Bazyl, O. K., Artyukhov, V. Y., and Mayer, G. V. (2020). Theoretical Study of Bisphenol A Photolysis. *Adv. Quan. Chem.* 81, 191–217. doi:10.1016/bs.aiq.2019.12.001
- Caffieri, S. (2002). Furocoumarin Photolysis: Chemical and Biological Aspects. *Photochem. Photobiol. Sci.* 1 (3), 149–157. doi:10.1039/B107329J
- Calvert, J. G., and Pitts, J. N. (1966). *Photochemistry*. New York: Wiley & Sons, 899.
- ChemOffice (2000). (*ChemDraw Ultra 6.0* и *Chem3D Ultra 6.0*). USA: Cambridge Corporation software. Available at: <http://www.cambridgesoft.com>.
- Dewar Michael, J. S. (2012). *Dougherty Ralph C. The PMO Theory of Organic Chemistry*. Boston: Springer US, 576.
- Dolan, L. C., Matulka, R. A., and Burdock, G. A. (2010). Naturally Occurring Food Toxins. *Toxins*. 2, 2289–2332. doi:10.3390/toxins2092289
- Garazd, Y. L., Garazd, M. M., Ogorodniichuk, A. S., and Khilya, V. P. (2006). Modified Coumarins. 24. Synthesis of Cycloheptane-Annellated Tetracyclic Furocoumarins. *Chem. Nat. Compd.* 42 (6), 656–664. doi:10.1007/s10600-006-0246-8
- Garazd, Y. L., Ogorodniichuk, A. S., Garazd, M. M., and Khilya, V. P. (2002). Modified Coumarins. 6. Synthesis of Substituted 5,6-Benzopsoralens. *Chem. Nat. Compounds*. 38 (5), 424–433. doi:10.1023/A:1022103524800
- Gasparro, F. P. (1996). Psoralen Photobiology: Recent Advances. *Photochem. Photobiol.* 63 (5), 553–557. doi:10.1111/j.1751-1097.1996.tb05654.x
- HyperChem 7.0 (2021). *HyperChem 7.0*. USA: Hypercube Inc. Available at: <http://www.hyper.com>.
- Ibrar, A., Khan, A., Ali, M., Sarwar, R., Mehsud, S., Farooq, U., et al. (2018). Combined *In Vitro* and *In Silico* Studies for the Anticholinesterase Activity and Pharmacokinetics of Coumarinyl Thiazoles and Oxadiazoles. *Front. Chem.* 6, 61. doi:10.3389/fchem.2018.00061
- Keuler, T., Gatterdam, K., Akbal, A., Lovotti, M., Marleaux, M., Geyer, M., et al. (2021). Development of Fluorescent and Biotin Probes Targeting NLRP3. *Front. Chem.* 9, 642273. doi:10.3389/fchem.2021.642273
- Lagey, K., Duinslaeger, L., and Vanderkelen, A. (1995). Burns Induced by Plants. *Burns*. 21, 542–543. doi:10.1016/0305-4179(95)00026-8
- Lai, T. I., Lim, B. T., and Lim, E. C. (1982). Photophysical Properties of Biologically Important Molecules Related to Proximity Effects: Psoralens. *J. Am. Chem. Soc.* 104 (26), 7631–7635. doi:10.1021/ja00390a039
- Liano, J., Raber, J., and Eriksson, L. A. (2003). Theoretical Study of Phototoxic Reactions of Psoralens. *J. Photochem. Photobiol. A: Chem.* 154 (2-3), 235–243. doi:10.1016/S1010-6030(02)00351-9
- Mantulin, W. W., and Song, P.-S. (1973). Excited States of Skin-Sensitizing Coumarins and Psoralens. Spectroscopic Studies. *J. Am. Chem. Soc.* 95 (16), 5122–5129. doi:10.1021/ja00797a004
- Mi, C., Ma, J., Wang, K. S., Zuo, H. X., Wang, Z., Li, M. Y., et al. (2017). Imperatorin Suppresses Proliferation and Angiogenesis of Human Colon Cancer Cell by Targeting HIF-1 α via the mTOR/p70S6K/4E-BP1 and MAPK Pathways. *J. Ethnopharmacology*. 203, 27–38. doi:10.1016/j.jep.2017.03.033
- Odyniec, M. L., Han, H.-H., Gardiner, J. E., Sedgwick, A. C., He, X.-P., Bull, S. D., et al. (2019). Peroxynitrite Activated Drug Conjugate Systems Based on a Coumarin Scaffold Toward the Application of Theranostics. *Front. Chem.* 7, 366. doi:10.3389/fchem.2019.00775
- Panno, M. L., and Giordano, F. (2014). Effects of Psoralens as Anti-Tumoral Agents in Breast Cancer Cells. *World J. Clin. Oncol.* 5, 348–358. doi:10.5306/wjco.v5.i3.348
- Parrish, J. A., Fitzpatrick, T. B., Tanenbaum, L., and Pathak, M. A. (1974). Photochemotherapy of Psoriasis With Oral Methoxsalen and Longwave Ultraviolet Light. *N. Engl. J. Med.* 291, 1207–1211. doi:10.1056/NEJM197412052912301
- Plotnikov, V. G. (1979). Regularities of the Processes of Radiationless Conversion in Polyatomic Molecules. *Int. J. Quan. Chem.* 16, 527–541. doi:10.1002/qua.560160311
- Pomogaev, V. A., and Artyukhov, V. Y. (2001). Spin-Orbital Interaction in Molecular Complexes of Naphthalene With Anthracene Derivatives. *J. Appl. Spectrosc.* 68 (2), 251–258. doi:10.1023/A:1019264118932
- Quirante, J. J. (1995). Study of the Bimolecular Pyrolysis of Acetic Acid by the Austin Model 1 Semi-Empirical Method. *J. Anal. Appl. Pyrolysis*. 31, 169–175. doi:10.1016/0165-2370(94)00822-1
- Rauhämäki, S., Postila, P. A., Niinivehmas, S., Kortet, S., Schildt, E., Pasanen, M., et al. (2018). Structure-Activity Relationship Analysis of 3-Phenylcoumarin-Based Monoamine Oxidase B Inhibitors. *Front. Chem.* 6, 41. doi:10.3389/fchem.2018.00041
- Reveguk, Z. V., Pomogaev, V. A., Kapitonova, M., Buglak, A. A., Kononov, A. I., et al. (2021). Structure and Formation of Luminescent Centers in Light-up Ag Cluster-Based DNA Probes. *J. Phys. Chem. C*. 124(18), 11129–11138. doi:10.1021/acs.jpcc.0c09973
- Scott, B. R., Pathak, M. A., and Mohn, G. R. (1976). Molecular and Genetic Basis of Furocoumarin Reactions. *Mutat. Research/Reviews Genet. Toxicol.* 39, 29–74. doi:10.1016/0165-1110(76)90012-9
- Shen, X., Liu, X., Wan, S., Fan, X., He, H., Wei, R., et al. (2019). Discovery of Coumarin as Microtubule Affinity-Regulating Kinase 4 Inhibitor that Sensitize Hepatocellular Carcinoma to Paclitaxel. *Front. Chem.* 7, 366. doi:10.3389/fchem.2019.00366
- Spreckelmeyer, S., van der Zee, M., Bertrand, B., Bodio, E., Stürup, S., and Casini, A. (2018). Relevance of Copper and Organic Cation Transporters in the Activity and Transport Mechanisms of an Anticancer Cyclometallated Gold(III) Compound in Comparison to Cisplatin. *Front. Chem.* 6, 377. doi:10.3389/fchem.2018.00377
- Stern, R. S. (2012). The Risk of Squamous Cell and Basal Cell Cancer Associated With Psoralen and Ultraviolet A Therapy: a 30-year Prospective Study. *J. Am. Acad. Dermatol.* 66, 553–562. doi:10.1016/j.jaad.2011.04.004
- Svetlichnyi, V. A. (2010). A Setup for Investigating the Absorption Spectra of Dyes in Excited States by the Pump-Probe Method Utilizing a Fluorescence Probe. *Instrum. Exp. Tech.* 53 (4), 575–580. doi:10.1134/S0020441210040196
- Tchaikovskaya, O. N., Bocharnikova, E. N., Sokolova, I. V., et al. (2020). Photophysical Processes in Coumarin Sensitizers. *Russ. Phys. J.* 63(8), 1339–1347. doi:10.1007/s11182-020-02176-3
- Wagstaff, D. J. (1991). Dietary Exposure to Furocoumarins. *Regul. Toxicol. Pharmacol.* 14, 261–272. doi:10.1016/0273-2300(91)90029-U
- Weber, M., Yamada, N., Tian, X., Bull, S. D., Minoshima, M., Kikuchi, K., et al. (2020). Sensing Peroxynitrite in Different Organelles of Murine RAW264.7 Macrophages With Coumarin-Based Fluorescent Probes. *Front. Chem.* 8, 39. doi:10.3389/fchem.2020.00039
- Wei, Y., Mei, L., Li, R., Liu, M., Lv, G., Weng, J., et al. (2018). Fabrication of an AMC/MMT Fluorescence Composite for its Detection of Cr(VI) in Water. *Front. Chem.* 6, 367. doi:10.3389/fchem.2018.00367
- Wrześniok, D., Beberok, A., Rok, J., Delijewski, M., Hechmann, A., Oprzondek, M., et al. (2017). UVA Radiation Augments Cytotoxic Activity of Psoralens in Melanoma Cells. *Int. J. Radiat. Biol.* 93, 734–739. doi:10.1080/09553002.2017.1297903
- Yañez, O., Osorio, M. I., Uriarte, E., Areche, C., Tiznado, W., Pérez-Donoso, J. M., et al. (2021). *In Silico* study of Coumarins and Quinolines Derivatives as Potent Inhibitors of SARS-CoV-2 Main Protease. *Front. Chem.* 8, 595097. doi:10.3389/fchem.2020.595097

Conflict of Interest: The authors declare that the research was conducted in the absence of any commercial or financial relationships that could be construed as a potential conflict of interest.

Publisher's Note: All claims expressed in this article are solely those of the authors and do not necessarily represent those of their affiliated organizations, or those of the publisher, the editors and the reviewers. Any product that may be evaluated in this article, or claim that may be made by its manufacturer, is not guaranteed or endorsed by the publisher.

Copyright © 2021 Tchaikovskaya, Dmitrieva, Bocharnikova, Chaidonova and Avramov. This is an open-access article distributed under the terms of the Creative Commons Attribution License (CC BY). The use, distribution or reproduction in other forums is permitted, provided the original author(s) and the copyright owner(s) are credited and that the original publication in this journal is cited, in accordance with accepted academic practice. No use, distribution or reproduction is permitted which does not comply with these terms.